Single-Site Mutations in the C-Terminal Domain of Bacteriophage λ *c*I Repressor Alter Cooperative Interactions between Dimers Adjacently Bound to O_R†

David S. Burz and Gary K. Ackers*

Department of Biochemistry and Molecular Biophysics, Washington University School of Medicine, St. Louis, Missouri 63110

Received February 2, 1994; Revised Manuscript Received April 29, 1994®

ABSTRACT: Wild-type *c*I repressor dimers bind with 2.5–3 kcal/mol of cooperative free energy to the tripartite right operator region (O_R) of bacteriophage λ [Johnson, A. D., et al. (1981) *Nature 294*, 217–223; Brenowitz, M., et al. (1986) *Methods Enzymol. 130*, 132–181]. Quantitative modeling has suggested that cooperativity is required for maintainence of the lysogenic state and for the efficient switch from lysogenic to lytic growth [Ackers, G. K., et al. (1982) *Proc. Natl. Acad. Sci. U.S.A. 79*, 1129–1133; Shea, M. A., & Ackers, G. K. (1985) *J. Mol. Biol. 181*, 211–230]. Cooperativity and self-association are thought to involve protein–protein contacts between C-terminal domains of the repressor molecule [Pabo, C. O., et al. (1979) *Proc. Natl. Acad. Sci. U.S.A. 76*, 1608–1612]. To address the importance of the C-terminal domain in mediating the cooperativity exhibited by λ *c*I repressor, a number of single-site mutant candidates were screened for possible deficiencies in cooperative interactions [Beckett, D., et al. (1993) *Biochemistry 32*, 9073–9079; Burz, D. S., et al. (1994) *Biochemistry 33*, 8399–8405]. Since repressor dimerization and binding to operator sites are coupled processes, elucidation of the energetic basis of regulation in this system requires that the equilibrium dimerization constants and the intrinsic and cooperative free energies of binding be measured. In this work we evaluate the interaction of eight mutant repressors with O_R DNA: Gly147→Asp (GD147), Pro158→Thr (PT158), Glu188→Lys (EK188), Lys192→Asn (KN192), Tyr210→His (YH210), Ser228→Arg (SR228), and Ser228→Asn (SN228), each with an amino acid substitution in the C-terminal domain, and Glu102→Lys (EK102) where the substitution lies in the "linker sequence" between domains. Self-assembly properties of six of these mutant repressors are presented in the preceding paper (Burz et al., 1994). In this work, the binding of mutant *c*I repressors to O_R was examined using quantitative DNAse I footprinting. This technique monitors individual site occupancy concurrent with binding at the other sites within a multisite complex. Simultaneous analysis of titration data for mutant repressors on wild-type and "reduced valency" O_R DNA shows that the intrinsic free energy of binding to individual operator sites for the mutants is essentially unchanged relative to that of wild type, while the magnitudes of cooperative DNA binding interactions fall into three general classes: WT, EK102, and SN228, which exhibit greater than ~2.5 kcal/mol of cooperative free energy; EK188 and SR228, which exhibit 1–2 kcal/mol of cooperativity; and GD147, KN192, and YH210, which are essentially devoid of cooperative binding free energy. The resultant deficiencies in cooperative interactions support the proposal that the origins of cooperativity may reside within the C-terminal domains. This detailed characterization of cooperativity mutants will facilitate ongoing *in vitro* studies regarding the molecular mechanism of regulation and *in vivo* studies aimed at elucidating the role of cooperativity in the life cycle of bacteriophage λ.

Understanding the molecular mechanism of biological regulation mediated by an ensemble of interacting components requires elucidation of the chemical and physical bases for the macromolecular interactions. Bacteriophage λ *c*I repressor binds with 2.5–3 kcal/mol of cooperative free energy to the tripartite right operator (O_R) of the phage genome [Johnson et al., 1979, 1981; for a review, see Ptashne (1986)]. Occupancy of operator sites by *c*I repressor and *cro* in O_R and O_L controls transcription from the promoters located within these two regions affording regulation of biological function (Ptashne et al., 1976; Sauer et al., 1979; Maurer et al., 1980; Meyer et al., 1980; Meyer & Ptashne, 1980). The biological activity resulting from interactions between *c*I repressor and *cro* with the right operator are shown in Figure 1. *c*I binds hierarchically, binding most tightly to O_R1, then to O_R2, and O_R3; binding of *cro* is tightest to O_R3 and weaker to sites O_R1 and O_R2. Occupancy of sites O_R1 and O_R2 by *c*I facilitates the constitutive production of *c*I from P_{RM} required for lysogenic growth and precludes transcription of *cro* off the right promoter, P_R (*i.e.*, P_{RM} "on", P_R "off"). Lytic growth is induced by *recA*-mediated degradation of *c*I monomers; this leads to derepression of P_R as O_R1 and O_R2 become vacant. Subsequent production of *cro* leads to occupancy of O_R3, shutting down transcription of *c*I (*i.e.*, P_R "on"; P_{RM} "off"). A model for gene regulation in which the distribution of microstate configurations involving occupancy of right operator

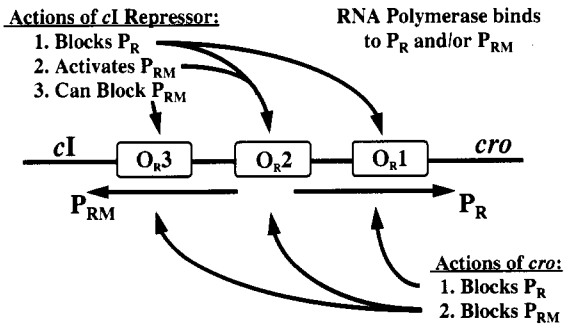

FIGURE 1: Biological activity resulting from interactions of *c*I and *cro* with O_R. Figure adapted from Shea and Ackers (1985).

† This work was supported by NIH Grants GM-39343 and R37-GM24486 (G.K.A.).

* Author to whom correspondence should be addressed.

® Abstract published in *Advance ACS Abstracts,* June 1, 1994.

0006-2960/94/0433-8406$04.50/0

sites by cI repressor is determined by equilibrium statistical thermodynamic probabilities suggests that *cooperative* binding of cI dimers is required for maintainence of the lysogenic state and for the efficient switch from lysogenic to lytic development (Ackers et al., 1982). This observation was further examined by coupling kinetic equations that describe the production of cI and *cro* with the equilibrium statistical thermodynamic model of site occupancy (Shea & Ackers, 1985). The model included positive autogenous regulation of cI production due to stimulation of RNA polymerase activity by cI occupancy of site O_R2 and simulated the onset of lytic growth by considering cI repressor degradation in the kinetic equation for cI production. Results corroborated the observation that cooperative binding of cI was necessary for the maintenance of lysogeny. Additional predictions of the model included the phenomenon of subinduction (*i.e.*, incomplete inactivation of repressor without lytic development; Bailone et al., 1979) and autogenous negative control of cI and *cro* transcription. The ability of the model to describe the biology of bacteriophage λ validates the use of statistical equilibrium thermodynamics to describe the interaction of cI repressor with O_R in order to regulate gene expression in this system.

Results from previous studies have provided a functional description of the domain structure for λ cI repressor; these include the following: (1) Intragenic complementation involving temperature-sensitive (ts) mutants of cI repressor suggests two distinct functional regions within the intact protein corresponding to subunit aggregation and DNA-binding ability (Lieb, 1966, 1976). (2) Papain-mediated cleavage of monomers yields two major fragments, an N-terminal polypeptide and a C-terminal fragment, corresponding to the two thermal transitions seen in the differential scanning calorimetric denaturation profile of intact repressor (Pabo et al., 1979). (3) The N-terminal fragment binds to specific λ operator sites (Sauer et al., 1979), noncooperatively (Johnson et al., 1979), and dimerizes with substantially weaker energetics than intact repressor (Weiss et al., 1987; Bain and Ackers, 1994), whereas the C-terminal domains are incapable of binding to operator DNA (Pabo et al., 1979). (4) Crystallographic analysis of co-crystals of the N-terminal fragment with operator DNA directly implicates that domain in specific contacts with DNA (Jordan & Pabo, 1988). (5) Electron microscopic observations of intact and DNA-bound repressor have revealed oligomers of tetrameric and higher order (Black & Pirotta 1975). (6) Sedimentation equilibrium studies suggest that the C-terminal fragments aggregate at concentrations at which the N-terminal fragments do not (Pabo et al., 1979). (7) Wild-type repressor self-associates to octamers at concentrations higher than 10^{-6} M (Senear et al., 1993). Collectively these studies have established the idea that while the N-terminal domain of cI repressor mediates protein–DNA interactions, the C-terminal domain is largely or exclusively responsible for the self-association properties which give rise to formation of the high-affinity binding species and for the cooperativity observed when dimers bind to adjacent operator sites.

The importance of cooperativity in the biological function of bacteriophage λ and the question of whether this function is sequestered within the C-terminal domain have not been accessible to direct experimental investigation because mutants defective in cooperative binding but competent in dimerization and local binding (*i.e.*, cooperativity mutants) have not, until recently, been available. One protein, GD147, was reported to exhibit a defective cooperativity phenotype (Beckett et al., 1993); however, that study did not incorporate the contribution of the monomer–dimer equilibrium of that mutant into the energetics of binding. Dimerization energetics for six mutant repressors were determined in the preceding paper (Burz et al., 1994). In this work, we report the interaction free energies of site-specific (intrinsic) and cooperative binding to O_R of eight single-site mutants of cI repressor. Results confirm that all are defective in one or more aspects of cooperative interactions, substantiating the idea that the C-terminal domain of cI repressor contains elements critical for regulation of biological function in the absence and presence of operator DNA. The results of this study lend further support to the use of the genetic screen reported in Beckett et al. (1993) as a useful tool for rapidly screening candidates for deficiencies in cooperative interactions. The broad spectrum of cooperativity and functional deficiencies exhibited by these mutant repressors will facilitate functional dissection *in vitro* of the oligomeric properties exhibited by this molecule as they relate to DNA binding and self-assembly, as well as *in vivo* studies aimed at elucidating the role of cooperativity in the life cycle of the bacteriophage.

EXPERIMENTAL PROCEDURES

Chemicals and Biochemical Materials. Ampicillin, bovine serum albumin (BSA), isopropyl β-D-thiogalactoside, lysozyme, Nonidet P-40, phenylmethanesulfonyl fluoride, polyethylenimine, and Sephadexes were from Sigma Chemical Co. Electrophoresis grade acrylamide, ammonium persulfate, bis(acrylamide), and TEMED were obtained from Bio-Rad, and Sequenal grade urea was from Pierce Chemical Co. or P.J. Cobert. Acrylamide, bis(acrylamide), and urea were deionized using Bio-Rad AG501-X8 mixed-bed resin prior to use.

α-^{32}P-Labeled deoxyribonucleotides (3000 Ci/mmol) were purchased from Amersham; unlabeled deoxyribonucleotides were from P-L Biochemicals. Restriction nucleases *Bgl*II, *Eco*RI, and *Pst*I were purchased from International Biotechnologies, Inc. (IBI). The large (Klenow) fragment of *E. coli* DNA polymerase I was obtained from Bethesda Research Labs (BRL) or IBI. Acetylated, nucleic acid enzyme grade BSA was from BRL, and calf thymus DNA (CT-DNA) was from P-L Biochemicals. Bovine pancreas deoxyribonuclease (DNase I, code D) was from Worthington.

Affi-Gel Blue affinity resin was from Bio-Rad. Extracti-Gel D resin was from Pierce or P.J. Cobert. Hydroxyapatite-Ultrogel (HAP-Ultrogel) was from IBF Biotechnics. Centriflo membrane cones (CF25) were from Amicon. Surfasil (silanizing agent) was from Pierce. All other chemicals were reagent or analytical grade.

Protein Purification. Repressors were overexpressed from the *tac* promoter on plasmid pEA300 (Amman et al., 1983) for wild type or on pFG600 (Gimble & Sauer, 1989) for the mutants (Beckett et al., 1993) and purified from *Escherichia coli* strain X90 as described (Johnson et al., 1980). The purification properties and yields of the mutant repressors were similar to those of wild type. All preparations were deemed >95% pure by Coomassie Brilliant Blue staining of samples electrophoresed on 8% SDS–polyacrylamide gels (Laemmli, 1970). Total monomer concentration of repressor was measured by UV absorbance at 280 nm, assuming an extinction coefficient of 1.18 mL mg^{-1} cm^{-1} (Sauer & Anderegg, 1978).

Total active monomer was calculated for each protein from stoichiometric titrations of O_R1 (see below) using nitrocellulose filter binding as described by Sauer (1979) and Johnson (1980)

at 5 °C in assay buffer [10 mM Bis–Tris (pH 7.0), 2.5 mM $MgCl_2$, 1 mM $CaCl_2$, 100 μg/mL BSA, and 2 μg/mL sonicated CT-DNA] containing 50 mM KCl, at an operator site concentration of 5 nM. Activities determined for each protein are as follows: wild type, 56%; EK102, 78%; GD147, 88%; PT158, 55%; EK188, 88%; KN192, 88%; YH210, 85%; SN228, 65%; SR228, 86%.

Preparation of Operator DNA. A 570-bp fragment of pO_R1, which contains the single operator site O_R1, was obtained by digestion with *Eco*RI. Excision of a 1107-bp fragment from plasmids containing wild type, pKB252 (O_R^+; Backman et al., 1976), and reduced-valency pBJ301 (O_R1^-), pBJ303 (O_R2^+), and pBJ306 (O_R2^-) of λ O_R was accomplished by restriction digestion with *Pst*I and *Bgl*II. pBJ301 contains the *vs*387 mutation (Ordal & Kaiser, 1973), which greatly reduces the affinity of repressor for O_R1. pBJ303 contains mutations *v*Cl and *v*C3, which reduce repressor binding for O_R1 and O_R3; pBJ306 exhibits reduced affinity for site O_R2 due to the *v*1 mutation (Meyer et al., 1980). Restriction digestion products were separated by electrophoresis on 1% agarose. The fragments were visualized by ethidium bromide staining, electroeluted, and passed over NACS Prepac columns (BRL). Operator DNA fragments were stored at –20 °C in 10 mM Tris-HCl (pH 7.2) and 0.1 mM EDTA (TE pH 7.2). Restriction fragments were labeled for binding by end-filling with [α^{32}P]dNTPs and the Klenow fragment of DNA polymerase I; excess free dNTPs were removed by passing the reaction mixture through two Select-D (G-50) spin columns (5′→3′, Inc.) and a NACS prepac column. A typical labeling reaction yields ~100 000 cpm/(picomole of DNA fragment). Labeled DNA was stored in TE, pH 7.2, at 4 °C at a concentration of ~1–2 pmol/mL and used within 2 weeks of preparation.

DNAse I Footprinting. Individual site binding isotherms were obtained by following the procedure for quantitative DNAse footprinting developed in this laboratory (Brenowitz et al., 1986). Reaction mixtures containing 20 000–30 000 cpm of end-labeled DNA were incubated in a total volume of 200 μL at 20 °C for 1–4 h prior to the digestion reaction. DNAse I was stored as a 2 mg/mL stock solution in 50 mM Tris-HCl (pH 7.2), 10 mM $MgCl_2$, 1 mM $CaCl_2$, 1 mM dithiothreitol, and 50% glycerol at –70 °C and diluted to the appropriate concentration into assay buffer less BSA and CT-DNA immediately prior to use. The final concentration of DNAse I and reaction time used in the footprinting experiments were 150 ng/mL for 1 min or 75 ng/mL for 2 min. Operator concentration was sufficiently low in all footprinting experiments to assume that $R_T = R + 2R_2$.

Two-dimensional optical scans of footprint autoradiographs were obtained using an Eikonix 1412 charge-coupled device (CCD) camera. Transmittance units obtained from the CCD camera were converted to optical density values relative to the output of the Aristogrid Model T light box used as a transmissive source for the optical scans. Optical density values were normalized to a 256 gray scale prior to use in the gel blocking program and calculation of fractional operator occupancy as previously described (Benowitz et al., 1986).

Analysis of Footprint Titrations. Energetic parameters for the interaction of *c*I repressor with the right operator were estimated using a nonlinear least-squares method (Johnson & Frasier, 1985). Analysis utilized expressions which separately consider dimer binding at individual operator sites. Quantitative expressions are constructed by considering the relative probability, f_s, of each operator configuration *s* (refer to Table 1):

Table 1: Microscopic Configurations and Associated Free Energy Contributions for the λ *c*I Repressor–Right Operator System[a]

	operator configurations						
species	O_R1		O_R2		O_R3	free energy contribution (ΔG_s)
1	0		0		0	reference state
2	R		0		0	ΔG_1
3	0		R		0	ΔG_2
4	0		0		R	ΔG_3
5	R	↔	R		0	$\Delta G_1 + \Delta G_2 + \Delta G_{12}$
6	R		0		R	$\Delta G_1 + \Delta G_3$
7	0		R	↔	R	$\Delta G_2 + \Delta G_3 + \Delta G_{23}$
8	R	↔	R	↔	R	$\Delta G_1 + \Delta G_2 + \Delta G_3 + \Delta G_{123}$

[a] Individual operator sites are denoted by 0 if vacant or by R if occupied by a repressor dimer. ↔ indicates pairwise interactions between bound dimers. ΔG_1, ΔG_2, or ΔG_3 is the intrinsic free energy of binding to individual sites; $\Delta G_{ij(k)}$ are free energies of interaction between bound dimers, defined as the difference in free energy change required to fill the sites simultaneously (ΔG_T) and the free energy change to fill them individually ($\sum_i \Delta G_i$). ΔG_s is the sum of contributions of the microscopic free energies for a given configuration. Free energies are related to the corresponding microscopic equilibrium constants, k_i, by the standard relationship $\Delta G_i = -RT \ln k_i$.

$$f_s = \frac{\exp(-\Delta G_s/RT)[R_2]^j}{\sum_s \exp(-\Delta G_s/RT)[R_2]^j} \quad (1)$$

where ΔG_s is the sum of contributions of the microscopic free energies corresponding to a given configuration (*s*), R_2 is the concentration of unbound repressor dimers, and *j* is the number of repressor dimers bound to an operator in the *s* configuration.

Simultaneous interaction of *c*I repressor with the three operator sites yields the configurations shown in Table 1. Fractional occupancy ($\bar{Y}i$) of individual sites is given by

$$\bar{Y}_1 = f_2 + f_5 + f_6 + f_8 \quad (2)$$

$$\bar{Y}_2 = f_3 + f_5 + f_7 + f_8 \quad (3)$$

$$\bar{Y}_3 = f_4 + f_6 + f_7 + f_8 \quad (4)$$

Binding expressions for mutant operators in which specific binding to one or more sites has been eliminated (reduced valency) are obtained in a similar manner. Intrinsic and cooperative free energies of interaction cannot be uniquely resolved from a single binding experiment using the wild-type operator O_R^+ due to the high correlation between ΔG_2 and the cooperative free energy terms (Senear et al., 1986). Simultaneous analysis of binding measurements performed on wild-type and reduced valency right operator DNA, in combination with the energetics of repressor dimerization, does permit resolution of all free energy terms (Senear et al., 1986; Koblan et al., 1992; Senear & Bolen, 1992). Normalized weighting factors were calculated to account for variations in experimental error by separately analyzing each footprint titration for the best phenomenological fit to the data; combinations of $\Delta G_{ij(k)}$ terms were used as input in the separate analyses; and ΔG_1, ΔG_2, ΔG_3, and the endpoints for each transition were fitted parameters. Following normalization of the individual isotherms, each experiment was refit; resultant variances from the best fit to combinations of $\Delta G_{ij(k)}$ terms were used to calculate weighting factors according to Bevington (1969). Duplicate experiments from each of four DNA operator templates were used in the final analysis. All calculations were performed on a Hewlett-Packard 9000 computer.

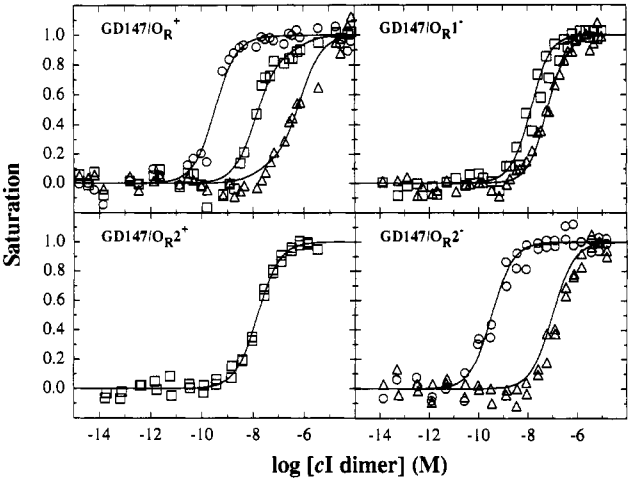

FIGURE 2: Isotherms resolved from simultaneous analysis of foot print titration data for GD147 binding to four O_R DNA templates. Free energies are given in Table 2. (○) Site O_R1; (□) site O_R2; (△) site O_R3.

RESULTS

DNAse I Footprint Titrations. Footprint titration data and best-fit curves from simultaneous analysis of GD147 binding to four DNA templates (O_R^+, O_R1^-, O_R2^-, O_R2^+) are shown in Figure 2. A broad range of concentrations were employed in order to unambiguously define the endpoints for the saturation transition obtained from raw data. This allows normalization of the individual curves to yield $\bar{Y}$, facilitating direct comparison of the binding isotherms and simultaneous analysis of the data. Intrinsic and cooperative free energies (Table 2) estimated from simultaneous analysis provide energetic parameters that satisfy data obtained for the eight binding isotherms shown in Figure 2. Resolved curves describe the data well for the interaction of GD147 with all templates, and this is typical of the quality of agreement obtained using the other mutant repressors of this study.

Isotherms resolved from simultaneous analysis of footprint titration data are shown for the interaction of wild-type and mutant repressors with O_R^+ in Figure 3. The dashed lines shown in the wild-type panel represent binding in the absence of cooperative interactions. Individual site binding curves obtained for GD147, EK188, KN192, YH210, and SR228 are qualitatively similar to one another but distinct from those obtained with wild type, EK102, and SN228. The most apparent difference is the absence of pronounced cooperative interactions between repressor dimers bound at sites O_R1 and O_R2, as indicated by (1) the increased steepness in the fitted isotherms and (2) the shift in position of the O_R1 and O_R2 transitions to lower dimer concentration. Resolved energetic parameters are summarized in Table 2. The intrinsic free

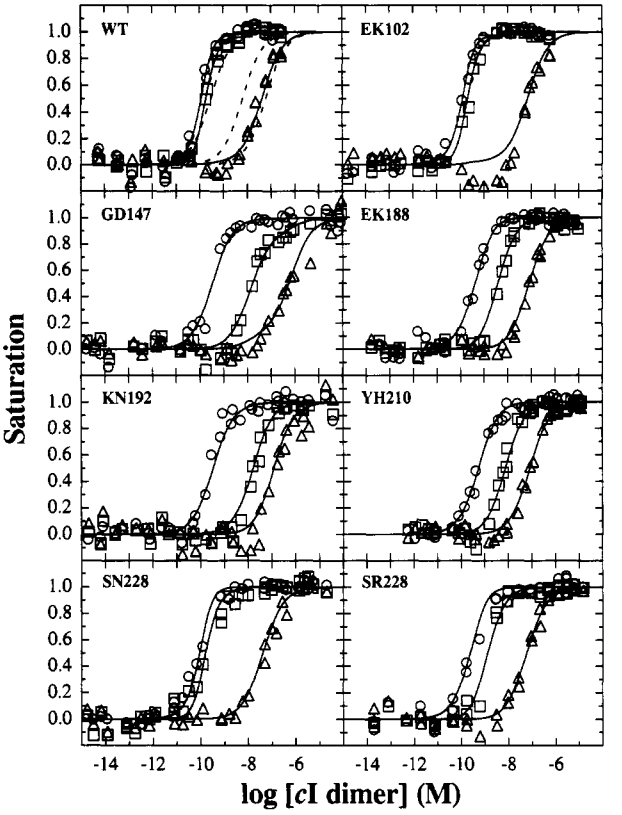

FIGURE 3: Isotherms resolved from simultaneous analysis of foot print protection data for wild-type and mutant cI repressor binding to O_R^+ template DNA. Free energies are given in Table 2. The dashed lines in the wild-type panel represent wild-type isotherms in the absence of cooperative interactions. (○) site O_R1; (□) site O_R2; (△) site O_R3.

energy of binding to O_R1 (ΔG_1) was found to be the same for each mutant and for the wild-type protein, consistent with the concept of a "pure cooperativity" mutant. Intrinsic binding of cI to O_R2 and O_R3 (ΔG_2, ΔG_3) was again the same for the mutant repressors but persistently weaker by ~0.5 kcal/mol relative to that of wild type. Cooperative free energies resolved for the mutant repressors are quite different from one another and, in general, completely different from those of wild type. Interaction parameters obtained for GD147, KN192, and YH210 indicate that cooperativity between repressor dimers bound at sites O_R1 and O_R2 is virtually eliminated by the single amino acid replacement; EK188 and SR228 show intermediate behavior with 1–1.5 kcal/mol for the ΔG_{12} interaction, while those of EK102 and SN228 are comparable to wild type. The trend is similar for the resolved pairwise cooperative free energy between sites O_R2 and O_R3: ΔG_{23} is ~0.5 kcal/mol for GD147, KN192, YH210, and SR228 and 1–2 kcal/mol for EK188 and SN228, while EK102 exhibits

Table 2: Resolved Free Energies of Interaction of Wild-Type and Mutant cI Repressor Dimers with Sites in λ O_R[a]

protein	ΔG_1[b]	ΔG_2	ΔG_3	ΔG_{12}	ΔG_{23}	ΔG_{123}	σ[c]
wild type	−12.8 ± 0.2	−11.0 ± 0.1	−9.7 ± 0.4	−2.6 ± 0.3	−3.3 ± 0.6	−2.8 ± 0.7	0.049
EK102	−12.8 ± 0.3	−10.5 ± 0.2	−9.2 ± 0.6	−3.0 ● 0.3	−4.5 ± 0.8	−3.4 ± 0.9	0.063
GD147	−12.7 ± 0.3	−10.5 ± 0.1	−9.4 ± 0.3	0.0 ± 0.5	−0.3 ± 0.4	1.1 ± 0.7	0.049
EK188[d]	−12.5 ± 0.1	−10.3 ± 0.1	−9.1 ± 0.2	−1.0 ± 0.2	−1.2 ± 0.4	−1.4 ± 0.4	0.047
KN192	−12.7 ± 0.2	−10.5 ● 0.1	−9.0 ± 0.3	0.1 ± 0.3	−0.6 ± 0.4	−0.2 ± 0.5	0.061
YH210	−12.4 ± 0.1	−10.5 ± 0.1	−9.4 ± 0.1	−0.4 ± 0.2	−0.5 ± 0.3	−0.5 ± 0.3	0.039
SN228	−13.0 ± 0.1	−10.4 ± 0.2	−9.4 ● 0.1	−3.2 ± 0.4	−1.9 ± 0.5	−3.7 ± 0.5	0.046
SR228	−12.8 ± 0.2	−10.6 ± 0.2	−9.2 ± 0.3	−1.4 ± 0.3	−0.7 ● 0.4	−1.9 ± 0.5	0.062

[a] The binding free energies were estimated from simultaneous analysis of O_R^+, O_R1^-, O_R2^-, and O_R2^+ footprint titration data. Dimerization constants used in the analyses are as follows: WT, 5.6 nM; EK102, 9.2 nM; GD147, 13.4 nM; KN192, 13.7 nM; YH210, 7.6 nM; SN228, 2.7 μM; SR228, 255 nM. [b] Standard Gibbs free energies in kcal/mol (with 67% confidence limits). [c] Square root of the variance of the fitted curves. [d] K_{dim} for EK 188 was assumed to be 10 nM.

Table 3: Resolved Free Energies of Interaction of Wild-Type and Mutant *c*I Repressor Monomers with Sites in λ O_R[a]

protein	ΔG_1[b]	ΔG_2	ΔG_3	ΔG_{12}	ΔG_{23}	ΔG_{123}	σ[c]
wild type	−11.5 ± 0.2	−10.3 ± 0.1	−9.1 ± 0.5	−2.1 ± 0.3	−2.7 ± 0.6	−2.4 ± 0.8	0.059
EK188	−11.4 ± 0.1	−9.6 ± 0.1	−8.5 ± 0.3	−0.9 ± 0.2	−1.2 ± 0.4	−1.4 ± 0.4	0.056
PT158	−10.9 ± 0.1	−9.7 ± 0.4	−9.1 ± 0.1	−2.4 ± 0.6	−2.6 ± 0.5	−2.1 ± 0.8	0.067

[a] The binding free energies were estimated from simultaneous analysis of O_R^+, O_R1^-, O_R2^-, and O_R2^+ footprint titration data. [b] Standard Gibbs free energies in kcal/(mol of monomer) (with 67% confidence limits). [c] Square root of the variance of the fitted curves.

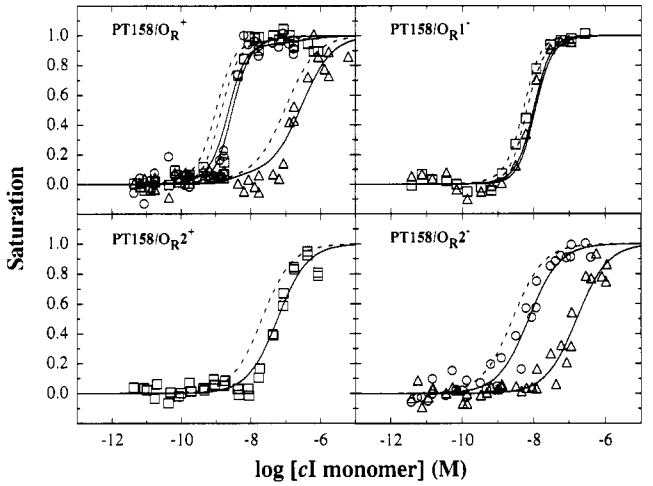

FIGURE 4: Isotherms resolved from simultaneous analysis of footprint titration data for PT158 binding to four O_R DNA templates as a function of total repressor monomer. The dashed lines represent wild-type isotherms in total repressor monomer. Free energies are given in Table 3. (○) Site O_R1; (□) site O_R2; (△) site O_R3.

an additional 1 kcal/mol of cooperative free energy relative to wild type. The cooperative free energy associated with overall binding to wild-type operator DNA, ΔG_{123} (Table 1), defines three classes of cooperativity mutants that track closely with values obtained for the pairwise interaction terms. GD147, KN192, and YH210 are essentially non-cooperative; EK188 and SR228 demonstrate intermediate cooperativity; and EK102 and SN228 are fully cooperative.

The value of the dimerization constant was not determined for EK188 due to experimental difficulties in isolating the ^{35}S-labeled repressor. An assumed value of 10 nM (−10.8 kcal/mol) for this interaction yielded intrinsic binding free energies comparable to those obtained for all of the other mutants, consistent with the assumption and observation that structural perturbation of the C-terminal domain does not substantially alter the intrinsic affinity of the repressor dimers for operator sites. This is supported by the energetics resolved for the interaction of EK188 with right operator DNA evaluated in total monomer concentration units (see Table 3 and below). Additional justification for this assumption is provided by the correlation between dimerization equilibrium constant and level of immunity conferred by this mutation in the genetic screen [*cf.* Beckett et al. (1993)]. By this criterion we would expect EK188 to dissociate in the nanomolar concentration range since reduced immunity is correlated with weaker dimerization (Burz et al., 1994). It is possible to estimate a value for ΔG_{dim} from the energetics resolved by analysis of binding data in monomer units (see below and Table 3); assuming that intrinsic binding is unaffected by the mutation, this yields a value of −10.4 ± 0.3 kcal/mole of monomer) for ΔG_{dim}.

Footprint Titrations of PT158. Results of the simultaneous analysis of footprint titrations of PT158 binding to O_R are shown in Figure 4. For comparison, isotherms resolved for wild-type binding are indicated by dashed lines. PT158 displays the hallmark of strong cooperative interactions as evidenced by the steepness of the fitted isotherms and the shift to lower concentrations in titrations of templates containing interacting *versus* noninteracting operator sites (*e.g.*, site O_R2 isotherm in O_R^+ *versus* O_R2^+). Analysis of binding data for this mutant was complicated by the fact that no dimeric species is detected up to ~1 μM in total protein (Burz et al., 1994). The footprint titrations of this study indicate that occupancy of both half-operator sites by PT158 occurs simultaneously; furthermore, these site-protection data show that O_R1 is occupied first, then O_R2, and then O_R3, as is observed for all of the other proteins studied. Using reduced-valency template DNA where the affinity of wild-type *c*I repressor dimers for a specific site is reduced or eliminated by point mutation, PT158 appears to bind as a dimer to viable operator sites; no half-site protection is observed under any conditions. Therefore, in the absence of a discernable dimer pool, DNA is inducing the assembly of dimers. The resolved free energies of interaction were estimated as a function of total monomer concentration and reported in kilocalories per mole of monomer in Table 3; for comparison, free energies estimated on the same basis are given for wild type and EK188. The conversion to monomer concentration units is equivalent to subtracting the contribution to the binding scheme of the linked dimerization reaction, and can be thought of as representing binding of two monomers to each operator site in the absence of a free dimer pool in accordance with the following thermodynamic cycle:

$$\begin{array}{ccc} nM_2 + O & \xleftrightarrow{\Delta G^{d}_{i(jk)}} & (M_2)_nO \\ \Delta G_{dim} \updownarrow & & \updownarrow \Delta G^{(DNA)}_{dim} \\ 2n(M_1) + O & \xleftrightarrow[\Delta G^{m}_{i(jk)}]{} & (M_1)_{2n}O \end{array}$$

where O represents operator DNA, M_1 is the *c*I repressor monomer, M_2 is the *c*I repressor dimer, n is the binding stoichiometry, ΔG_{dim} is the monomer–dimer equilibrium free energy for free repressor, $\Delta G^{d}_{i(jk)}$ is the free energy for dimer binding to operator DNA, $\Delta G^{m}_{i(jk)}$ is the free energy for binding of two monomers to an operator site, and $\Delta G^{(DNA)}_{dim}$ is the free energy of DNA-induced dimer formation. The cooperative free energy values shown in Table 3 are slightly more positive from those reported in Table 2 [kcal/(mol of dimer)]; intrinsic free energies, however, differ significantly, reflecting the linked contribution of dimerization to the binding process. The pattern of intrinsic binding to sites O_R1 and O_R2 being ~0.5 kcal/mol weaker than that of wild type persists with the exception of SN228; the weak dimerization expressed by this mutant propagates into the intrinsic free energy resolved for those sites (not shown). The inability of PT158 to form discrete dimers allows evaluation of the strength of DNA-induced conformational changes on the protein. Assuming that the intrinsic operator affinity of (DNA-induced) PT158 dimers is identical to that of wild-type dimers, an assumption validated by the results obtained for all of the

Table 4: Comparison of the Sums of the Loading and Model-Dependent Resolved Free Energies for Wild-Type and Mutant *c*I Monomer Binding to O_R1^- and O_R^+ DNA[a]

	(O_R1^-)		(O_R^+)	
protein	$\Sigma\Delta G_L$[b]	$\Sigma\Delta G_{i(j)}$[c]	$\Sigma\Delta G_L$[d]	$\Sigma\Delta G_{i(jk)}$[e]
wild type	−20.5	−22.1 ± 1.2	−32.5	−33.3 ± 1.6
EK102	−22.4	−22.0 ± 1.7	−32.6	−32.7 ± 1.9
GD147	−18.6	−19.0 ± 0.8	−27.6	−29.2 ± 1.4
PT158	−21.2	−21.5 ± 1.1	−33.1	−31.7 ± 1.5
EK188	−19.7	−19.3 ± 0.8	−30.7	−30.9 ± 0.9
KN192	−18.0	−18.9 ± 0.8	−28.9	−30.1 ± 1.1
YH210	−18.9	−19.3 ± 0.5	−30.4	−30.7 ± 0.6
SN228	−18.5	−18.3 ± 1.0	−30.1	−29.5 ± 1.1
SR228	−17.6	−18.6 ± 0.8	−29.3	−30.0 ± 1.1

[a] The loading free energy is obtained by numerical integration of the binding data for each set of templates. $\Delta G_{L,i} = RT \int \ln X \, dY_i$. All values are in kcal/(mol of monomer). [b] Sum of loading free energies $\Delta G_{L,2}$ and $\Delta G_{L,3}$ calculated by integration of the combined data sets obtained using O_R1^- template DNA. [c] Sum of the model-dependent resolved free energy contributions for binding to O_R1^- template DNA ($\Delta G_2 + \Delta G_3 + \Delta G_{23}$). Error is the sum of errors associated with each estimated parameter. [d] Sum of loading free energies $\Delta G_{L,1}$, $\Delta G_{L,2}$, and $\Delta G_{L,3}$ calculated by integration of the combined data sets obtained using O_R^+ template DNA. [e] Sum of the model-dependent resolved free energy contributions for binding to O_R^+ template DNA ($\Delta G_1 + \Delta G_2 + \Delta G_3 + \Delta G_{123}$). Error is the sum of errors associated with each estimated parameter.

mutant repressors examined in this study (refer to Table 2), a DNA-induced dimerization free energy can be estimated for PT158 binding to O_R in accordance with the linkage scheme presented above. This calculation suggests that the DNA-induced dimerization free energy could be as great as −9.5 ± 0.3 kcal/mol for binding at site O_R1 and −11 kcal/mol for binding at site O_R3.

Loading Free Energies. Individual site loading free energies (Ackers et al., 1983) were calculated by numerical integration of binding data obtained from duplicate experiments performed using each DNA template. Such model-independent evaluation of binding data provides an alternate assessment of the free energy changes observed in cooperative systems in two ways: (1) the total free energy change exhibited by repressor binding to a given DNA template should be the same when evaluated by the two methods; (2) the distribution of free energy in a multisite system should result in a greater share of the cooperative energy being partitioned to the weaker of two interacting sites (Ackers et al., 1983). Repressor dimer binding to O_R2^- and O_R2^+ templates exhibits no cooperative interactions. Therefore the calculated loading and resolved intrinsic free energies are the same (not shown). The sum of loading free energies determined by integration of titration data from O_R^+ and O_R1^- titrations (*e.g.*, $\Delta G_{L,1} + \Delta G_{L,2} + \Delta G_{L,3}$ and $\Delta G_{L,2} + \Delta G_{L,3}$) is compared with the sum of the intrinsic and cooperative free energies resolved for binding to the same templates in Table 4. The total free energy changes obtained by both methods of evaluation are in good agreement. Combining data sets improved the quality of integration, but inherent experimental noise precluded assessment of the error associated with $\Delta G_{L,i}$, as well as the distribution of cooperative free energy to individual sites. Previous estimates of comparable data vary from 0.3 to 0.8 kcal/mol for each operator site (Senear & Ackers, 1990; Koblan & Ackers, 1992).

Population Distribution of Microstates. The population distribution of the microconfigurations (f_i) in Table 1, as a function of total monomer, is shown in Figure 5 for representatives of the fully cooperative (wild type), intermediate (SR228), and non-cooperative (KN192) classes of *c*I repressor. Probabilities were calculated using the free energy values resolved from simultaneous analysis of binding data in

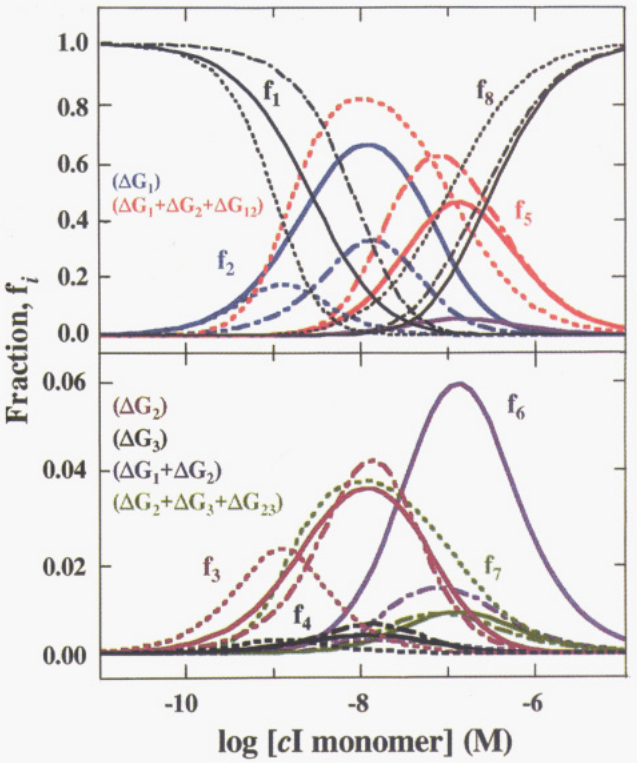

FIGURE 5: Population distribution of the species shown in Table 1 as a function of total *c*I monomer. Dashed lines, wild type; discontinuous lines, SR228; solid lines, KN192. Panel A (top): Species comprising greater than 10% of the population. Panel B (bottom): Species comprising less than 10% of the population.

kilocalories per mole of monomer. Aside from the disappearance of f_1, the unligated reference state, and the appearance of f_8, the fully ligated species, two species dominate the distribution for each repressor: Singly ligated species, f_2 (ΔG_1), and doubly ligated species, f_5 ($\Delta G_1 + \Delta G_2 + \Delta G_{12}$), constitute peak fractional occupancy, respectively, of 20–60% and 45–80%, over the course of saturating O_R (panel A). As cooperativity increases, f_5 constitutes a larger percentage of the total population of species, whereas f_2 exhibits a decreasing contribution to the overall population; concurrently the maxima for f_5 shift to lower protein concentration, reflecting the increase in total free energy associated with the cooperative system relative to the non-cooperative one. In addition, f_6 ($\Delta G_1 + \Delta G_3$), which represents less than 1% (peak) of the population in fully cooperative repressors, increases to ~10% for non-cooprative repressors (GD147, KN192, YH210). The remaining species (panel B), f_7 ($\Delta G_2 + \Delta G_3 + \Delta G_{23}$), increases slightly for the highly cooperative repressors (WT, EK102, PT158), while singly ligated f_3 (ΔG_2) and f_4 (ΔG_3) do not vary appreciably as a function of cooperativity and do not represent a significant contribution to the total population of species. The distribution of dimeric species tracks with that of monomers but is scaled to the strength of the dimerization reaction. Assuming the same level of expression of total protein for the mutants as for wild type, the species' population shows a marked dependence with regard to both dimerization and cooperativity. These results demonstrate that the species distribution of the cooperativity mutants reflects different modes of interaction of repressors with operator DNA, and thus regulation of the life cycle of the bacteriophage. The energetic significance of this assumption can be explored by calculating population distributions for different permutations of the triply ligated microstate, for example, to examine

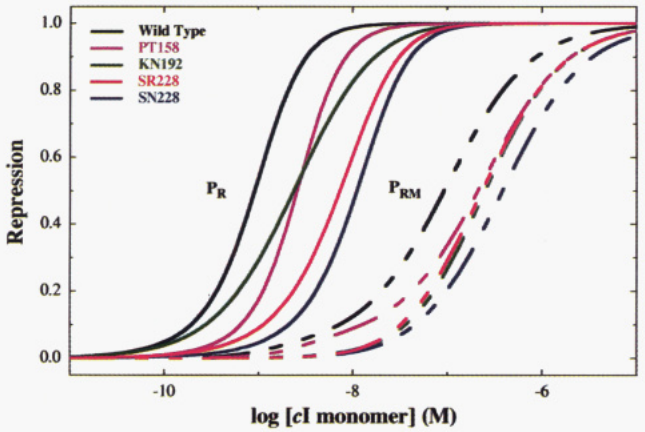

FIGURE 6: Predicted repression curves for wild-type and mutant *c*I repressors. Solid lines represent repression of P_R, discontinuous lines represent repression of P_{RM}.

the consequences of exclusive pairwise cooperative interactions in the fully ligated operator.

Repression Curves. Repression curves calculated for P_R and P_{RM}, using the energetic terms resolved for five repressors (wild type, PT158, KN192, SN228, and SR228) in kilocalories per mole of monomer, are shown in Figure 6. EK102 is predicted to behave much like wild-type repressor, and the curves for KN192, GD147, YH210, and EK188 are quite similar to one another. Occupancy of sites O_R1 and O_R2 by *c*I will contribute to P_R repression, whereas occupancy of site O_R3 will promote repression of P_{RM}. Linear combinations of the probabilities described in Table 1 were used to generate repression curves (Ackers et al., 1982):

$$f(P_{RM}) = f_2 + f_3 + f_5 + f_6 + f_7 + f_8 \quad (5)$$

$$f(P_R) = f_4 + f_6 + f_7 + f_8 \quad (6)$$

The range of midtransition values predicted for P_R and P_{RM} spans approximately 1 order of magnitude in protein concentration; wild type is at the extreme low end of the spectrum for both promoters. These calculatuions do not consider promoter activity *per se*, but whether or not RNA polymerase can bind to the promoter site [see Shea and Ackers (1985)]. At a concentration where wild-type *c*I repressor has completely repressed P_R, most of the C-terminal domain mutants are predicted to result in slight derepression of P_R (solid lines). The effects at P_{RM} are similar: at a monomer concentration that predicts 50% derepression of P_{RM} by wild-type *c*I repressor, mutant repressor binding produces 65–80% derepression of that promoter (dashed lines). Since repressor monomers expressing weakened dimerization energetics require much higher concentrations of total protein in order to occupy operator sites, one might predict that the strength of the linked dimerization equilibrium is foremost in promoter repression. On the other hand, partitioning of cooperative free energy to sites O_R1 and O_R2, whose occupancy will facilitate repression of P_R, shifts the curves to lower concentrations. A repressor that binds to O_R with wild-type intrinsic free energy and no cooperativity (*e.g.*, KN192) will result in a P_R transition curve that is shifted to higher protein concentration relative to wild type; the steepness of the transition, however, is much greater for the cooperative species. Conversely, repressors exhibiting similar cooperative free energy but weakened dimerization will yield repression transitions at higher protein concentrations (*e.g.*, wild type *vs* SN228). Repression at P_{RM} is less dependent on ΔG_{dim} since at the midpoint concentration of these repression curves enough dimer is available for binding. SN228 and GD147 are exceptions to this; SN228 dimerization occurs in the micromolar concentration range, while GD147 is shifted to higher total protein concentration due to the positive value resolved for the ΔG_{123} interaction (curve not shown; refer to Table 2). Furthermore, the effects of free energy partitioning to site O_R3 are minimized because the population of species containing an occupied site O_R3 is greatly subdued throughout the course of saturation (preceding section).

Values for the intrinsic free energies resolved for the mutant proteins can be scaled to reflect the weaker intrinsic binding expected at 37 °C. A monotonic but nonlinear decrease in intrinsic binding as a function of temperature is observed with wild-type repressor, such that extrapolation of wild-type data requires that ΔG_1, ΔG_2, and ΔG_3 be increased by 0.7, 0.2, and 0.7 kcal/(mole of dimer) (Table 2; Koblan & Ackers 1992) while the cooperative terms remain essentially unchanged. Calorimetric measurements currently underway in this labortory suggest that the thermal behavior of GD147 and wild type are not parallel (E. Merabet, this laboratory, unpublished experiments); this suggests that linear extrapolation of Gibbs energies is likely to be an oversimplification and that measurements of binding free energies and dimerization will have to be determined for the mutant protein in question prior to quantitative modeling of data acquired at this temperature.

Model Dependence of the Binding Data. Binding obtained from footprint titration experiments using mutant repressors provides an extended database for examining the interaction of *c*I repressor with O_R. The proteins studied exhibit discrete operator-bound species distributions that differ exclusively in the resolved cooperative free energies. Simultaneous analysis of binding data employing models of microconfiguration distributions that differ only in the manner in which cooperative free energy is distributed in the triply liganded state may provide evidence of alternate binding modes. Referring to Table 1, the first seven species are common to all models considered and specify pairwise interactions between dimers bound to adjacent sites (f_5,f_7). The alternate-pairwise model ascribes a ΔG_{12} interaction to the triply liganded state, whereas the reverse alternate-pairwise model allows only a ΔG_{23} interaction; the extended-pairwise model allows both ΔG_{12} and ΔG_{23} interactions. The general model invokes a ΔG_{123} interaction in which the cooperative free energy is distributed in a nonspecified manner in the triply liganded state, while the "fully general" model includes an additional ΔG_{13} parameter that ascribes an interaction between dimers bound at sites O_R1 and O_R3. Holding all cooperative terms equal to 0 in the simultaneous analysis treats the system as if it were noncooperative and does not describe the binding data except that for the fully noncooperative proteins. Floating the interaction terms consistently yields values for $\Delta G_{ij(k)}$ in the range from 0 to –4 kcal/(mole of dimer), supporting the idea that positive cooperativity occurs for the remaining mutants during the course of loading O_R.

Cooperative interactions may be affected by occupancy of reduced-valency sites. ΔG_{12} is defined for a vacant O_R3 site; if O_R3 is occupied, then $\Delta G_{1'2'}$ represents the strength of this interaction. Similar arguments can be made for ΔG_{23} and $\Delta G_{2'3'}$, and for ΔG_{13} and $\Delta G_{1'3'}$. Attempts to fit binding data to the general model consistently returned a value of 0 for ΔG_{13}, thus ruling out the need to consider this type of interaction and, thus, the fully general model. Likewise, demonstrating that ΔG_{23} does not change during the course of fitting the data obtained from binding to O_R1^- and O_R^+ eliminates the need to invoke a $\Delta G_{2'3'}$ term. An exception to this exists in the case of GD147 (see below); in this instance,

ΔG_{23} does not equal $\Delta G_{2'3'}$, but since ΔG_{12} is equal to 0, using the general model ΔG_{123} effectively describes the interaction denoted by $\Delta G_{2'3'}$.

Initial formulation of the alternate-pairwise model used to quantitatively describe the interaction of wild-type *c*I repressors with right operator DNA (Ackers et al., 1982) was based on the observation that site O_R3 bound *c*I cooperatively in the absence of a viable O_R1 site (Johnson et al., 1979). As alluded above, this observation has a minimal physiological effect due to suppression of species containing only occupied O_R2 and O_R3 sites during the course of loading the wild-type operator. The model dependence of wild-type repressor dimer binding to O_R as a function of pH was evaluated by Senear and Ackers (1990), where it was concluded that (1) the general model consistently provided best fits to the experimental data, (2) the extended-pairwise model also adequately described the data over most of the pH range studied, and (3) best fits to the alternate-pairwise model showed systematic deviations from the titration data.

No such model dependence of the resolved free energies could be discerned for EK188, KN192, YH210, and SR228. However, a best fit to the titration data obtained for GD147 and SN228 could only be obtained using the general model described in Table 1, in order to account for deviations when analyzed according to the alternate-pairwise model. Analyses of the GD147 titration data by both models support the conclusion that cooperative binding of dimers to sites O_R1 and O_R2 is eliminated. Results for SN228 suggest that the cooperative interaction denoted by ΔG_{23} predominates more so with this mutant than with the wild-type repressor in the triply ligated configuration. Binding of the highly cooperative EK102 could not be fit adequately using the alternate-pairwise model but, like wild type binding, adhered to the tenets of the extended pairwise, reverse alternate-pairwise, and general models.

The general model best describes the data overall despite the fact that the resolved free energy terms and standard deviations do not change appreciably when the titration data are analyzed using alternative models (not shown). Deviations are especially evident in the fitted curve through site O_R3 in titrations of the wild-type operator and likely result from lack of sufficient data at high concentration to resolve the upper endpoint for that isotherm. Since wild-type repressor titration curves are adequately fit using the extended-pairwise model, the inability of that model to describe mutant binding data suggests that these proteins may exhibit alternate binding configurations differing from those inferred for wild type. In order to determine exactly which model best describes the *c*I–O_R interaction, data with a standard error substantially less than the best obtained in this study (*i.e.*, ~4%) must be obtained.

DISCUSSION

Ongoing goals of this laboratory include elucidation of the molecular mechanism which gives rise to the cooperativity observed when *c*I repressor dimers bind to O_R and evaluation of the importance of these cooperative interactions in the regulation of the life cycle of bacteriophage λ. The initial phase of the current study involved the inception of a genetic screen to isolate C-terminal domain single-site mutants of *c*I repressor with possible defects in cooperative interactions (Beckett et al., 1993). Since a cooperativity mutant candidate might be defective in its ability to dimerize and/or bind to O_R, complete characterization of the interactions between *c*I repressor and O_R requires that the energetics of dimerization as well as the intrinsic and cooperative free energies of binding be determined [refer to Figure 1 in Burz et al. (1994)]. A thermodynamic approach characterizes energetically significant interactions regardless of the origin of the structural complexity. Dimerization free energies were measured in the preceding paper (Burz et al., 1994) using analytical gel chromatography. In this work, quantitative DNAse I footprint titrations were used to resolve Gibbs binding energies; combining data obtained from wild-type and reduced-valency mutant operator templates permits resolution of the energetics of each macromolecular interaction, thereby facilitating assessment of the role of cooperativity in the regulation of the ensemble.

Mutant repressors were isolated in an attempt to test the assumption that the regulatory elements required for cooperative binding to DNA and for self-assembly were confined to the C-terminal domain. This assumption was borne out by two observations: (1) The genetic screen used by Benson et al. (1994) resulted in isolation of spontaneous mutants whose amino acid substitutions were confined to the C-terminal domain. (2) All of the genetically screened repressors studied that contained a C-terminal domain replacement showed altered cooperativity. An exception to this is the PT158 mutation, which was originally isolated by Gimble and Sauer (1989) as an *ind*$^+$ mutant showing increased susceptibility to *recA*-mediated degradation. The single mutation isolated outside of the C-terminal domain, EK102, lies in the linker between domains and behaves much like the wild-type repressor.

Analyses of footprint titrations yielded a broad range of interaction free energies for the mutant repressors, ranging from no change in the interaction free energy relative to wild type (e.g., ΔG_{12} in SN228) to the total elimination of interaction free energy (e.g., ΔG_{12} in GD147 and KN192); refer to Table 2. Superficially these observations implicate all of the replaced sites or residues as being required for cooperativity *via* either alteration of charge, as had been suggested for GD147 (Beckett et al., 1993); steric or positional effects (see below); or specific protein–protein side-chain interactions involving intra- or intermolecular domain contacts. Binding isotherms obtained using aged (nicked) DNA templates exhibited significant specific hypersensitivity to DNAse I digestion that is coupled to operator site occupancy (not shown). The hypersensitive sites were located immediately adjacent to and within operator binding sites. Kinetic artifacts and interaction of DNAse I with bound repressor were ruled out by varying the exposure of the ensemble to DNAse I. Hypersensitivity was observed only for the non-cooperative repressors GD147, KN192, and to a lesser extent SR228; the effect was not observed in wild-type or EK102 binding to O_R. These observations imply that changes in DNA conformation may occur concomitant with operator binding. Incremental loss of cooperative free energy (1.2 ± 0.3 and 2.6 ± 0.4 kcal/mol for ΔG_{12}) suggests that the DNA may be limiting configurational fluctuations that accompany the binding of mutant dimers that cannot interact with operator sites in a manner similar to wild type. The intrinsic free energy of mutant repressor binding to sites O_R2 and O_R3 is consistently weaker relative to that of wild type by about 0.5 kcal/mol. This is the case even for EK102, which lies in the linker region between domains. Allosteric communication mediated by protein–protein contacts involving residues from either or both domains as well as the linker region could be responsible for this small but persistent difference. The intrinsic free energy of N-terminal domain (residues 1–102) binding to O_R2 and

Table 5: Summary of Cooperative Energetics and Assembly States of Wild-Type and Mutant *c*I Repressors

protein	dimerization constant (nM)[a]	stoichiometry of self-assembly[b]	relative cooperativity[c]
wild type	5.6	1:2:8[d]	+++
EK102	9.2	1:2:>6[e]	++++
GD147	13	1:2[e,f]	0
PT158	n/a[h]	1:>6[e]	++
EK188	n/d[h]	2:>6[e,g]	+
KN192	14	1:2[e,f]	0
YH210	7.6	1:2[e,f]	0
SN228	2700	1:2[e]	+++
SR228	260	1:2[e,f]	+

[a] Preceding paper (Burz et al., 1994). [b] 1 = monomer, 2 = dimer, etc. [c] Average resolved free energies (Tables 2 and 3); + = ~1 kcal/mol. [d] Senear et al. (1993). [e] T. Laue, personal communication. [f] This laboratory, unpublished. [g] See text; see also the preceding paper (Burz et al., 1994). [h] n/a, not applicable; n/d, not determined.

O_R3 demonstrates the same change in free energy, lending support to this hypothesis (Bain and Ackers, 1994). Characterization of more cooperativity mutants will be required in order to shed light on the emerging patterns associated with functional changes accompanying structural perturbation.

Dimerization of *c*I monomers is functionally linked to operator binding but not to cooperativity. Evidence for this is supported by two sets of observations (refer to Table 5): First, three repressor mutants that are severely deficient in their ability to self-associate (PT158, SN228, and SR228) express intermediate or full cooperativity. The deficiency in dimerization does not alter intrinsic affinity for operator sites, nor does it uniformly affect cooperative binding of dimers to O_R. Second, mutants that dimerize with energetics comparable to wild type display a spectrum of cooperative free energies. The former point is clarified by comparing the dimerization free energy and the resolved cooperative free energies for SN228 and SR228. SN228 dimerizes 3.5 kcal/mol less strongly than wild type yet binds to O_R1 and O_R2 with wild-type cooperativity; SR228 dimerizes 2 kcal/mol less strongly and exhibits a 40% reduction in ΔG_{12} relative to wild type. Similarly, cooperative binding to O_R2 and O_R3 is reduced by 40% and 90%, respectively, for SN228 and SR228. This differential effect on self-association and cooperative binding to operator DNA facilitates decoupling of the two processes and further suggests that position 228 may lie along both energy transduction pathways.

No compelling pattern of functional perturbation is evident as a result of introduction of a charged amino acid side chain into the C-terminal domain structure: The mutants EK102 and EK188 (+2 charge difference) exhibit full and intermediate cooperativity, YH210 and SR228 (+1 charge difference) have no and intermediate cooperativity, and GD147 and KN192 (−1 charge difference) are non-cooperative. In addition, there is no correlation with replacement of native residues by larger amino acids that might be expected to introduce steric restrictions on interactions involving mutated side chains: EK102, GD147, EK188, and SR228 display the full spectrum of observed cooperative interactions. Last, positional effects are indirectly implicated in all of the mutant proteins examined. However, the only strong candidates for direct positional effect mutations are PT158, SN228, and SR228 [see below and Burz et al. (1994)]; in these cases the ability of repressor monomers to dimerize is either eliminated or greatly weakened. Proline is known to present significant energetic barriers to biological processes; an example would be proline isomerization rate limited folding reactions. Additionally, the position of a proline residue within a folded polypeptide chain lends a distinct structural characteristic which is frequently required to maintain a correct structure for biological activity. Replacing such a structurally critical residue might be expected to have an adverse effect on optimal biological function. Replacement of serine by arginine appears to disrupt the tertiary structure of dimers more so than asparagine replacement concurrent with a reduction in cooperativity, but SR228 dimerizes more strongly than the fully cooperative SN228 repressor. Since SN228 was fit adequately using the model described in Table 1, whereas SR228 exhibited no model-dependent fit to its binding isotherms, the inability to describe binding of the residue 228 mutants to O_R using similar models suggests that they interact differently with operator DNA from one another despite their binding with identical intrinsic free energies. Stokes radii determined from chromatography experiments indicate that all of the mutant dimers examined, with the exception of SN228, are 2–3 Å larger than wild-type dimers; SN228 dimers are the same size as wild-type dimers. The increase in size is observed only for the mutant repressors that are defective in cooperative operator binding [Table 3 in Burz et al. (1994)].

SN228 was independently isolated by Hochschild and Ptashne (1988), who inferred from footprint protection experiments that this protein was noncooperative in binding to O_R. There is insufficient data to substantiate this conclusion, as it has been shown that in order to obtain a measure of the cooperativity associated with repressor binding to right or left operator DNA, footprints must be performed using both wild-type and reduced-valency mutant operator templates (Senear et al., 1986). The authors also observed that higher concentrations of SN228 than of wild type were required to saturate a single operator site (O_R1), but took into account neither the activity of the mutant repressor, which was cited as being "relatively low" and "undetermined", nor the possibility that the protein was defective in its ability to dimerize. SN228 was found to bind less tightly to a single operator site (O_R1) as well as to tandem operator sites (O_R1^-) when assayed using nitrocellulose filter binding (Beckett et al., 1993). Since SN228 has been shown to bind to specific sites in O_R with no significant alteration in intrinsic free energy, the explanation of these observations lies in the inability of the molecule to form sufficent high affinity binding species across the range of concentrations used in those experiments due to a defect in dimerization coupled with a reduced activity of the protein. These findings underscore the need for complete characterization of a new protein in order to interpret physical data. GD147 was previously isolated by Gimble and Sauer (1985, 1986) as a mutation that resists *recA*-mediated cleavage (*ind*$^-$). Phage containing this mutant repressor exhibit a higher rate of spontaneous induction and make less turbid plaques than phage containing wild-type repressor, consistent with the idea that the cooperative interactions eliminated in GD147 are responsible for the properties observed *in vivo*, and substantiating the implication of the studies presented in Johnson et al. (1979) and Shea and Ackers (1985) that cooperative DNA binding is essential for maintaining the lysogenic state and regulating the onset of lytic development.

Characterization of the stoichiometric relationships for self-association of *c*I repressor monomers from their dimeric to their octameric forms with only a low abundance of tetramers has been reported recently (Senear et al., 1993). The authors suggested that octamers may bind to the three-site operator and that the apparent cooperativity observed at "local sites" might be a manifestation of DNA-promoted intraoctameric interactions rather than the current model of independently

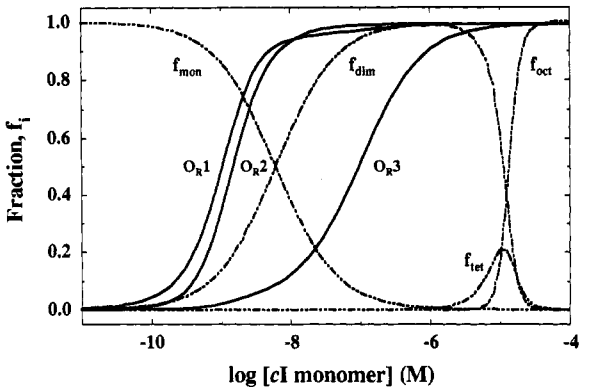

FIGURE 7: Fraction of repressor species present as a function of total protein, over the course of loading right operator sites O_R1, O_R2, and O_R3 with wild-type cI repressor: f_{mon}, fraction of cI monomers, f_{dim}, fraction of cI dimers; f_{tet}, fraction of cI tetramers; f_{oct}, fraction of cI octamers. Equilibrium free energy values used to calculate the species populations are as follows: Monomer–dimer, −11 kcal/(mole of monomer) (Burz et al., 1994); dimer–tetramer, −7 kcal/(mole of tetramer) (Senear et al., 1993); tetramer–octamer, −23 kcal/(mole of octamer) (Senear et al., 1993).

binding dimers that interact with each other (Ackers et al., 1982). A prediction of this hypothesis would be that a mutant repressor which is incapable of forming octamers should be incapable of cooperative binding to multisite operator DNA. Our observations suggest that there is no correlation between formation of higher order oligomers and cooperative DNA binding; for example, SR228 and SN228 do not aggregate beyond dimers, yet they display intermediate and fully cooperative binding, respectively, to right operator DNA (Table 5). At the concentration of wild-type cI repressor monomer estimated to be present in a lysogenic cell (~200 nM; Chadwick et al., 1973; Sauer, 1979), there is a large stable pool of dimers and a minimal pool of monomers and octamers (see Figure 7). A steep octamer-assembly transition coupled with a small increase in concentration will favor formation of octamers at the expense of the dimer pool; similarly, a decrease in cI concentration will result in an increase in the monomer pool. The dimer–octamer transition reported for wild-type cI monomers by Senear et al. (1993) occurs from ~1 to 100 μM with a free energy of −23 kcal/(mole of octamer) [−2.9 kcal/(mole of monomer)], while repressor saturation of right operator sites occurs at submicromolar concentration. If octamers were capable of binding directly to the three-site operator in a variety of modes that would leave vacant the exact combinations of sites measured by footprint titration, the fact that the concentration range for appreciable octamer formation is greater than the concentration range where the lysogenic to lytic switch occurs argues that they would never come into play in a physiologically significant way. As shown in Figure 7, oligomerization of repressor dimers, therefore, will have no effect on the footprint titration isotherms reported in this study since the experiments performed did not exceed 5 μM in total repressor. When we extend the titration range to ~10–50 μM total protein, apparent deprotection of saturated operator sites by repressors that aggregates beyond dimers is observed (*i.e.*, WT, EK102, EK188, and PT158; Burz et al., 1994), whereas repressors that do not exhibit higher order aggregation maintain a state of operator saturation. Furthermore, since monomers can apparently be induced to dimerize by DNA (*i.e.*, PT158), whereas octamers cannot, formation of octamers may represent a means of regulating site occupancy at extreme cI repressor concentrations by depopulating specific sites and/or by acting as "storage forms" (Pirotta et al., 1970) to help provide a constant source of dimers as a buffer against lytic development, possibly playing a role in the phenomenon of subinduction. Relationships between formation of octamers or higher order assemblies of λ cI repressor and binding to O_R will be presented elsewhere.

The cooperativity mutants identified in this study will facilitate a systematic analysis of the importance of cooperativity in the λ system. GD147, KN192, and YH210 are ideal candidates for quantitative evaluation of the importance of cooperativity *in vivo*. These molecules exhibit properties required of pure cooperativity mutants, *i.e.*, no appreciable change in intrinsic binding to operator sites or dimerization relative to wild-type cI repressor and virtual elimination of cooperative interactions between dimers bound to adjacent sites on DNA. Decoupling dimerization and DNA binding will facilitate physical and chemical studies on the molecular details of operator–protein recognition in λ phage. The results described in this and the preceding paper (Burz et al., 1994) define a spectrum of functional deficiencies involving cI repressor dimerization, higher order oligomerization, and cooperative binding to right operator DNA (Table 5). In all repressors studied the intrinsic binding to operator sites is largely unaffected by mutation, except for the slight increase in intrinsic free energy of binding to sites O_R2 and O_R3. This effect may result from the disruption of tertiary structure, as evidenced by changes in hydrated radius as a result of single-site replacement, and suggests that communication between domains may play a fundamental role in regulating the biological function of cI repressor.

ACKNOWLEDGMENT

The authors wish to acknowledge Robert T. Sauer for the EK102, GD147, PT158, and SN228 mutants used in this study and for his role in developing the genetic screen used to examine all mutant cI repressor candidates for defects in cooperative interactions. We also extend our thanks to Phillip Youderian for contributing the mutant repressors KN192, EK188, YH210, and SR228 used in the genetic screening assay and in this study. We thank Tom Laue for preliminary estimations of assembly states of the mutant repressors by sedimentation equilibrium.

REFERENCES

Ackers, G. K., Johnson, A. D., & Shea, M. A. (1982) *Proc. Natl. Acad. Sci. U.S.A. 79*, 1129–1133.
Ackers, G. K., Shea, M. A., & Smith, F. R. (1983) *J. Mol. Biol. 170*, 223–242.
Amann, E., Brosius, J., & Ptashne, M. (1983) *Gene 25*, 167–178.
Backman, K. C., Ptashne, M., & Gilbert, W. (1976) *Proc. Natl. Acad. Sci. U.S.A. 73*, 4174–4178.
Bailone, A., Levine, A., & Devoret, R. (1979) *J. Mol. Biol. 131*, 655–661.
Bain, D., & Ackers, G. K. (1994) *Biochemistry* (in press).
Beckett, D., Burz, D. S., Ackers, G. K., & Sauer, R. T. (1993) *Biochemistry 32*, 9073–9079.
Benson, N., Adams, C., & Youderian, P. (1994) *Mol. Microbiol. 11*, 567–579.
Bevington, P. R. (1969) in *Data Reduction and Error Analysis for the Physical Sciences*, McGraw-Hill, New York.
Brack, C., & Pirrotta, V. (1975) *J. Mol. Biol. 96*, 139–152.
Brenowitz, M., Senear, D. F., Shea, M. A., & Ackers, G. K. (1986) *Methods Enzymol. 130*, 132–181.
Burz, D. S., Ackers, G. K., & Beckett, D. (1993) *7th Gibbs Conference on Biological Thermodynamics*, p 12, Carbondale, IL.
Burz, D. S., Beckett, D., Benson, N., & Ackers, G. K. (1994) *Biochemistry* (preceding paper in this issue).

Chadwick, P., Pirrotta, V., Steinberg, R., Hopkins, N., & Ptashne, M. (1973) *Cold Spring Harbor Symp. Quant. Biol. 35*, 283–294.
Gimble, F. S., & Sauer, R. T. (1985) *J. Bacteriol. 162*, 147–154.
Gimble, F. S., & Sauer, R. T. (1986) *J. Mol. Biol.* 192, *39*–47.
Gimble, F. S., & Sauer, R. T. (1989) *J. Mol. Biol. 206*, 29–39.
Hochschild, A., & Ptashne, M. (1988) *Nature 336*, 353–357.
Johnson, A. D. (1980) Ph.D. Thesis, Harvard University, Cambridge, MA.
Johnson, A. D., Meyer, B. J., & Ptashne, M. (1979) *Proc. Natl. Acad. Sci. U.S.A. 76*, 5061–5065.
Johnson, A. D., Pabo, C. O., & Sauer, R. T. (1980) *Methods Enzymol. 65*, 839–856.
Johnson, A. D., Poteete, A. R., Lauer, G., Sauer, R. T., Ackers, G. K., & Ptashne, M. (1981) *Nature 294*, 217–223.
Johnson, M. L., & Frasier, S. G. (1985) *Methods Enzymol. 117*, 301–342.
Jordan, S. R., & Pabo, C. O. (1988) *Science 242*, 893–899.
Koblan, K. S., & Ackers, G. K. (1991) *Biochemistry 30*, 7817–7821.
Koblan, K. S., & Ackers, G. K. (1992) *Biochemistry 31*, 57–65.
Koblan, K. S., Bain, D. L., Beckett, D., Shea, M. A., & Ackers, G. K. (1992) *Methods Enzymol. 210*, 405–425.
Laemmli, U. (1970) *Nature 227*, 680–685.
Lieb, M. (1966) *J. Mol. Biol. 16*, 149–163.
Lieb, M. (1976) *MGG, Mol. Gen. Genet. 146*, 291–297.
Maurer, R., Meyer, B. J., & Ptashne, M. (1980) *J. Mol. Biol. 139*, 147–161.
Meyer, B. J., & Ptashne, M. (1980) *J. Mol. Biol. 139*, 195–205.
Meyer, B. J., Maurer, R., & Ptashne, M. (1980) *J. Mol. Biol. 139*, 162–194.
Ordal, G. W., & Kaiser, A. D. (1973) *J. Mol. Biol. 79*, 709–722.
Pabo, C. O., Sauer, R. T., Sturtevant, J. M., & Ptashne, M. (1979) *Proc. Natl. Acad. Sci. U.S.A. 76*, 1608–1612.
Ptashne, M. (1986) in *A Genetic Switch, Gene Control and Phage* λ, Cell Press, Cambridge, MA, and Blackwell, Palo Alto, CA.
Ptashne, M., Backman, K., Humayun, M. Z., Jeffrey, A., Maurer, R., Meyer, B., & Sauer, R. T. (1976) *Science 194*, 156–161.
Sauer, R. T. (1979) Ph.D. Thesis, Harvard University, Cambridge, MA.
Sauer, R. T., & Anderegg, R. (1978) *Biochemistry 17*, 1092–1100.
Sauer, R. T., Pabo, C. O., Meyer, B. J., Ptashne, M., & Backman, K. C. (1979) *Nature 279*, 396–400.
Senear, D. F., & Ackers, G. K. (1990) *Biochemistry 29*, 6568–6577.
Senear, D. F., & Bolen, D. W. (1992) *Methods Enzymol. 210*, 463–481.
Senear, D. F., Brenowitz, M., Shea, M. A., & Ackers, G. K. (1986) *Biochemistry 25*, 7344–7354.
Senear, D. F., Laue, T. M., Ross, J. B. A., & Waxman, E. (1993) *Biochemistry 32*, 6179–6189.
Shea, M. A., & Ackers, G. K. (1985) *J. Mol. Biol. 181*, 211–230.
Weiss, M. A., Pabo, C. O., Karplus, M., & Sauer, R. T. (1987) *Biochemistry 26*, 897–904.